



$\pi\pi$ scattering from low to high energy

Gilberto Colangelo

u^b

^b
UNIVERSITÄT
BERN

Bangalore, India, January 13. 2009

Outline

Introduction

Roy equations

Chiral symmetry + dispersive methods

Comparison to lattice and experiment

Extension of the Roy equation analysis*

Phenomenological inputs

D and F waves

Constraints on high-energy behaviour

Summary

* Work in progress together with Irinel Caprini and Heiri Leutwyler

Outline

Introduction

Roy equations

- Chiral symmetry + dispersive methods

- Comparison to lattice and experiment

Extension of the Roy equation analysis*

- Phenomenological inputs

- D and F waves

- Constraints on high-energy behaviour

Summary

Why is $\pi\pi$ scattering interesting

- ▶ the pions are the quasi-Goldstone bosons of spontaneous chiral symmetry breaking of QCD
- ▶ $m_{u,d}/\Lambda_{\text{QCD}} \sim \text{percent} \Rightarrow$ precise predictions within the effective field theory method are possible
- ▶ $\pi\pi$ scattering is special also from the S-matrix point of view: at low energy dispersion relations and unitarity relate this amplitude only to itself, also in the crossed channels
- ▶ this implies that the two scattering lengths (subtractions constants) are the essential parameters at low energy
- ▶ conversely, many other observables are influenced by the $\pi\pi$ interaction in intermediate or final states (e.g. $K \rightarrow 2\pi, 3\pi, \eta \rightarrow 3\pi, (g-2)_\mu$)

Low-energy theorem for $\pi\pi$ scattering

$\mathcal{M}(\pi^0\pi^0 \rightarrow \pi^+\pi^-) \equiv A(s, t, u)$ = isospin invariant amplitude

Low energy theorem: $A(s, t, u) = \frac{s - M^2}{F^2} + \mathcal{O}(p^4)$ Weinberg 1966

$$M^2 = B(m_u + m_d) \quad M_\pi^2 = M^2 + \mathcal{O}(m_q^2), \quad F_\pi = F + \mathcal{O}(m_q)$$

All physical amplitudes can be expressed in terms of $A(s, t, u)$

$$T^{l=0} = 3A(s, t, u) + A(t, s, u) + A(u, t, s) \Rightarrow T^{l=0} = \frac{2s - M_\pi^2}{F_\pi^2}$$

S wave projection ($l=0$)

$$t_0^0(s) = \frac{2s - M_\pi^2}{32\pi F_\pi^2} \quad a_0^0 = t_0^0(4M_\pi^2) = \frac{7M_\pi^2}{32\pi F_\pi^2} = 0.16$$

Chiral predictions for a_0^0 and a_0^2

Quark mass dependence of M_π and F_π :

$$M_\pi^2 = M^2 \left(1 - \frac{M^2}{32\pi^2 F^2} \bar{\ell}_3 + O(M^4) \right)$$

$$F_\pi = F \left(1 + \frac{M^2}{16\pi^2 F^2} \bar{\ell}_4 + O(M^4) \right)$$

Phenomenological determinations ([indirect](#)):

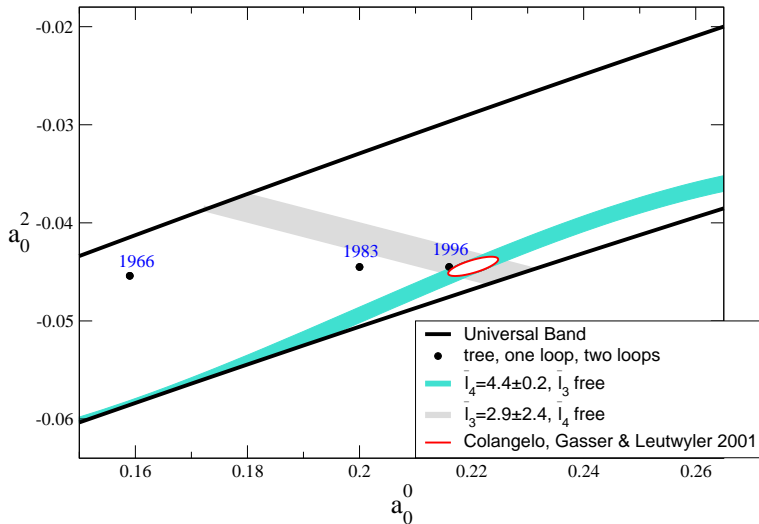
$$\bar{\ell}_3 = 2.9 \pm 2.4$$

Gasser & Leutwyler (84)

$$\bar{\ell}_4 = 4.4 \pm 0.2$$

GC, Gasser & Leutwyler (01)

Lattice calculations determine these constants **directly**

Chiral predictions for a_0^0 and a_0^2 

Higher orders

Higher order corrections are suppressed by $\mathcal{O}(M_\pi^2/\Lambda^2)$

$\Lambda \sim 1 \text{ GeV} \Rightarrow$ **expected to be a few percent**

$$a_0^0 = 0.200 + \mathcal{O}(p^6) \quad a_0^2 = -0.0445 + \mathcal{O}(p^6)$$

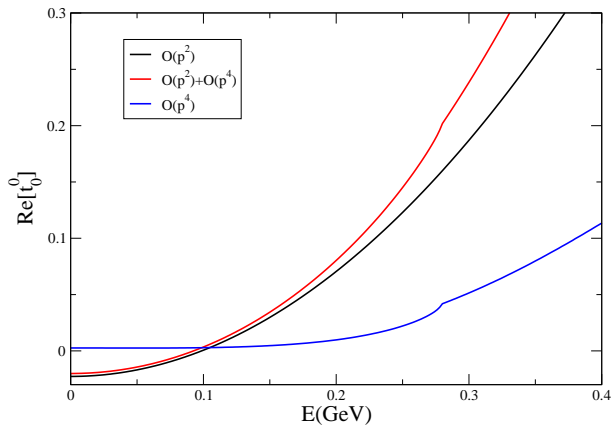
The reason for the rather large correction in a_0^0 is a chiral log

$$a_0^0 = \frac{7M_\pi^2}{32\pi F_\pi^2} \left[1 + \frac{9}{2} l_x + \dots \right] \quad a_0^2 = -\frac{M_\pi^2}{16\pi F_\pi^2} \left[1 - \frac{3}{2} l_x + \dots \right]$$

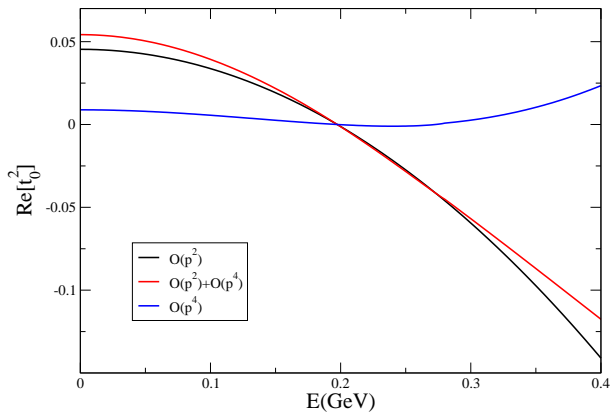
$$l_x = \frac{M_\pi^2}{16\pi^2 F_\pi^2} \ln \frac{\mu^2}{M_\pi^2}$$

Gasser and Leutwyler (84)

Higher orders



Higher orders



Outline

Introduction

Roy equations

Chiral symmetry + dispersive methods

Comparison to lattice and experiment

Extension of the Roy equation analysis*

Phenomenological inputs

D and F waves

Constraints on high-energy behaviour

Summary

Roy equations

Unitarity effects can be calculated **exactly** using dispersive methods

Unitarity, analyticity and crossing symmetry \equiv **Roy equations**
S.M. Roy (71)

Numerical solutions of the Roy equations

Pennington-Protopopescu, Basdevant-Froggatt-Petersen (70s)

Ananthanarayan, GC, Gasser and Leutwyler (00)

Descotes-Genon, Fuchs, Girlanda and Stern (01)

Input: S- and P-wave imaginary parts above 0.8 GeV

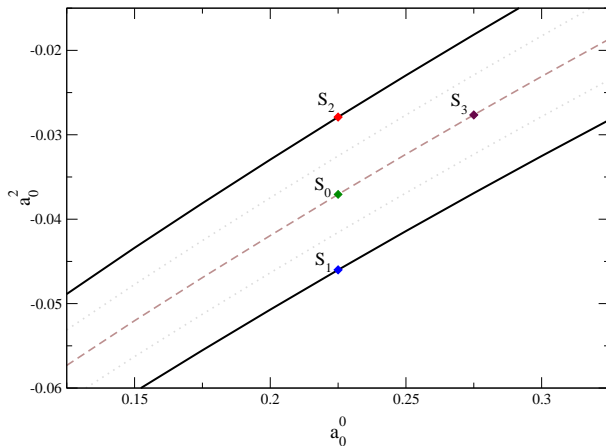
imaginary parts of all higher waves

two subtraction constants, e.g. a_0^0 and a_0^2

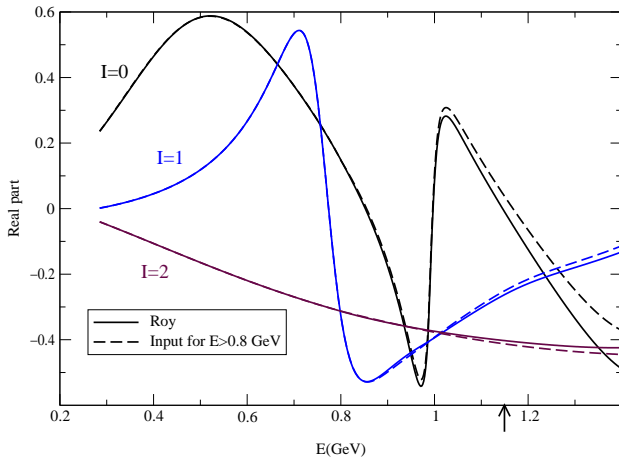
Output: the full $\pi\pi$ scattering amplitude below 0.8 GeV

Note: a_0^0, a_0^2 inside the universal band \Rightarrow the solution is unique

Numerical solutions



Numerical solutions



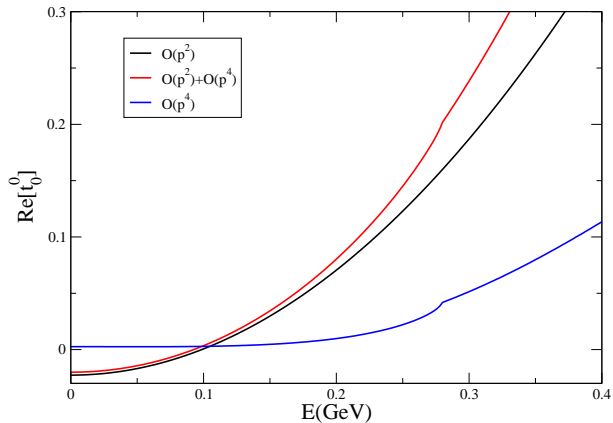
Combining CHPT and dispersive methods

In CHPT the two subtraction constants are **predicted**

Subtracting the amplitude at threshold (a_0^0, a_0^2) is not **mandatory**

The freedom in the choice of the subtraction point can be exploited to use the chiral expansion where it converges best, *i.e.* **below threshold**

Combining CHPT and dispersive methods



Combining CHPT and dispersive methods

The convergence of the series at threshold is greatly improved if CHPT is used only below threshold

CHPT at threshold

$$\begin{array}{rccccccc} a_0^0 & = & 0.159 & \rightarrow & 0.200 & \rightarrow & 0.216 \\ 10 \cdot a_0^2 & = & -0.454 & \rightarrow & -0.445 & \rightarrow & -0.445 \\ & & p^2 & & p^4 & & p^6 \end{array}$$

Combining CHPT and dispersive methods

The convergence of the series at threshold is greatly improved if CHPT is used only below threshold

CHPT at threshold

$$\begin{array}{rcccl}
 a_0^0 & = & 0.159 & \rightarrow & 0.200 & \rightarrow & 0.216 \\
 10 \cdot a_0^2 & = & -0.454 & \rightarrow & -0.445 & \rightarrow & -0.445 \\
 & & p^2 & & p^4 & & p^6
 \end{array}$$

CHPT below threshold + Roy solutions

$$\begin{array}{rcccl}
 a_0^0 & = & 0.197 & \rightarrow & 0.2195 & \rightarrow & 0.220 \\
 10 \cdot a_0^2 & = & -0.402 & \rightarrow & -0.446 & \rightarrow & -0.444
 \end{array}$$

GC, Gasser and Leutwyler (01)

Final results

$$\begin{aligned}a_0^0 &= 0.220 \pm 0.001 + 0.009\Delta l_4 - 0.002\Delta l_3 \\10 \cdot a_0^2 &= -0.444 \pm 0.003 - 0.01\Delta l_4 - 0.004\Delta l_3\end{aligned}$$

$$\text{where } \bar{l}_4 = 4.4 + \Delta l_4 \quad \bar{l}_3 = 2.9 + \Delta l_3$$

Adding errors in quadrature

$$[\Delta l_4 = 0.2, \Delta l_3 = 2.4]$$

$$\begin{aligned}a_0^0 &= 0.220 \pm 0.005 \\10 \cdot a_0^2 &= -0.444 \pm 0.01 \\a_0^0 - a_0^2 &= 0.265 \pm 0.004\end{aligned}$$

Final results

$$\begin{aligned} a_0^0 &= 0.220 \pm 0.001 + 0.009\Delta l_4 - 0.002\Delta l_3 \\ 10 \cdot a_0^2 &= -0.444 \pm 0.003 - 0.01\Delta l_4 - 0.004\Delta l_3 \end{aligned}$$

$$\text{where } \bar{l}_4 = 4.4 + \Delta l_4 \quad \bar{l}_3 = 2.9 + \Delta l_3$$

Adding errors in quadrature

$$[\Delta l_4 = 0.2, \Delta l_3 = 2.4]$$

$$\begin{aligned} a_0^0 &= 0.220 \pm 0.005 \\ 10 \cdot a_0^2 &= -0.444 \pm 0.01 \\ a_0^0 - a_0^2 &= 0.265 \pm 0.004 \end{aligned}$$

Peláez and Ynduráin have criticized these results

Claim 1: our input above 1.4 GeV is not correct (PY 03)

The criticism has been answered (Caprini *et al.* 03)

Final results

$$\begin{aligned} a_0^0 &= 0.220 \pm 0.001 + 0.009\Delta l_4 - 0.002\Delta l_3 \\ 10 \cdot a_0^2 &= -0.444 \pm 0.003 - 0.01\Delta l_4 - 0.004\Delta l_3 \end{aligned}$$

$$\text{where } \bar{l}_4 = 4.4 + \Delta l_4 \quad \bar{l}_3 = 2.9 + \Delta l_3$$

Adding errors in quadrature

$$[\Delta l_4 = 0.2, \Delta l_3 = 2.4]$$

$$\begin{aligned} a_0^0 &= 0.220 \pm 0.005 \\ 10 \cdot a_0^2 &= -0.444 \pm 0.01 \\ a_0^0 - a_0^2 &= 0.265 \pm 0.004 \end{aligned}$$

Peláez and Ynduráin have criticized these results

Claim 2: our calculation for $\langle r^2 \rangle_s$ is not correct (Y, 04)

The criticism has been answered (Ananthanarayan *et al.* 04)

Lattice determination of $\bar{\ell}_3$ and $\bar{\ell}_4$

- ▶ the theoretical prediction relies on **dispersion relations** and **chiral symmetry** for fixing the two subtraction constants
- ▶ Low-energy theorem for the $\pi\pi$ scattering amplitude

$$A(s, t, u) = \frac{s - M^2}{F^2} + \mathcal{O}(p^4) \longrightarrow \frac{s - M_\pi^2}{F_\pi^2} + \mathcal{O}(p^4)$$

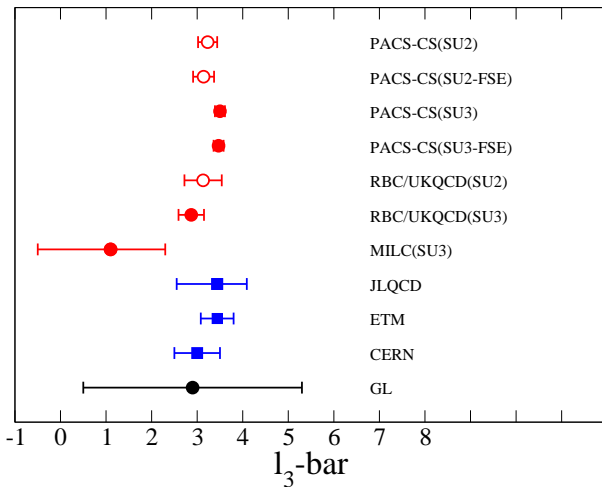
- ▶ the two subtraction constants are essentially given by M_π and F_π , **up to higher order corrections** (which matter and have been taken into account) – the most important ones are:

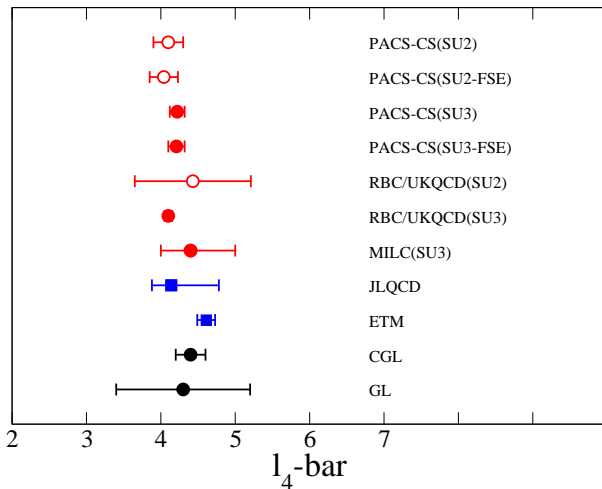
$$M_\pi^2 = M^2 \left(1 - \frac{M^2}{32\pi^2 F^2} \bar{\ell}_3 + \mathcal{O}(M^4) \right)$$

$$F_\pi = F \left(1 + \frac{M^2}{16\pi^2 F^2} \bar{\ell}_4 + \mathcal{O}(M^4) \right)$$

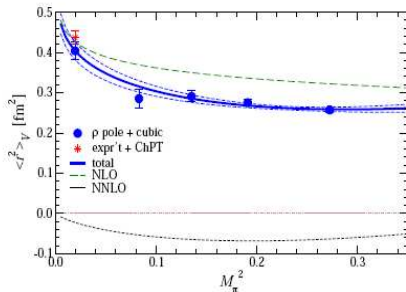
Lattice determination of \bar{l}_3 and \bar{l}_4

group	ChPT	\bar{l}_3	\bar{l}_4
$N_f = 2 + 1$			
PACS-CS	SU(2) no FV	3.23(21)	4.10(20)
	SU(2) FV	3.14(23)	4.04(19)
	SU(3) no FV	3.50(11)	4.22(10)
	SU(3) FV	3.47(11)	4.21(11)
RBC/UKQCD	SU(3)	2.87(28)	4.10(5)
	SU(2)	3.13(33)(24)	4.43(14)(77)
MILC	SU(3)	1.1(6) $\begin{pmatrix} +1.0 \\ -1.5 \end{pmatrix}$	4.4(4) $\begin{pmatrix} +4 \\ -1 \end{pmatrix}$
$N_f = 2$			
JLQCD	SU(2)	3.44(57) $\begin{pmatrix} +0 \\ -68 \end{pmatrix}$ $\begin{pmatrix} +32 \\ -0 \end{pmatrix}$	4.14(26) $\begin{pmatrix} +49 \\ -0 \end{pmatrix}$ $\begin{pmatrix} +32 \\ -0 \end{pmatrix}$
ETM	SU(2)	3.44(8)(35)	4.61(4)(11)
CERN	SU(2)	3.0(5)(1)	—
pheno			
CGL	SU(2)	2.9(2.4)	4.4(2)

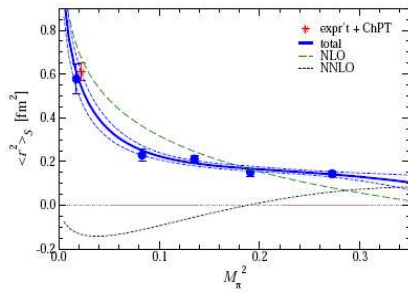
Lattice determination of \bar{l}_3 and \bar{l}_4 

Lattice determination of \bar{l}_3 and \bar{l}_4 

Scalar and charge radius of the pion – JLQCD/TWQCD



● dof = 6, $\chi^2/\text{dof} = 1.3$



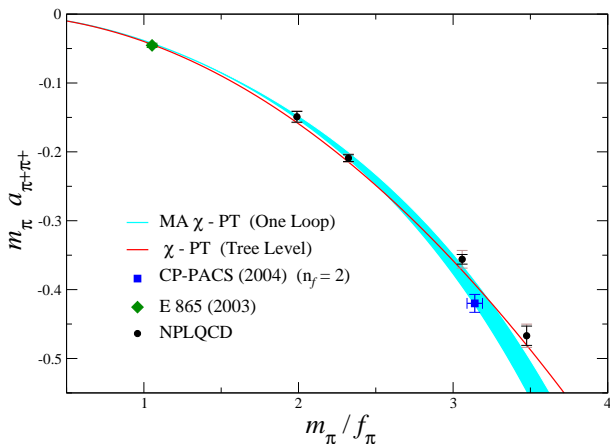
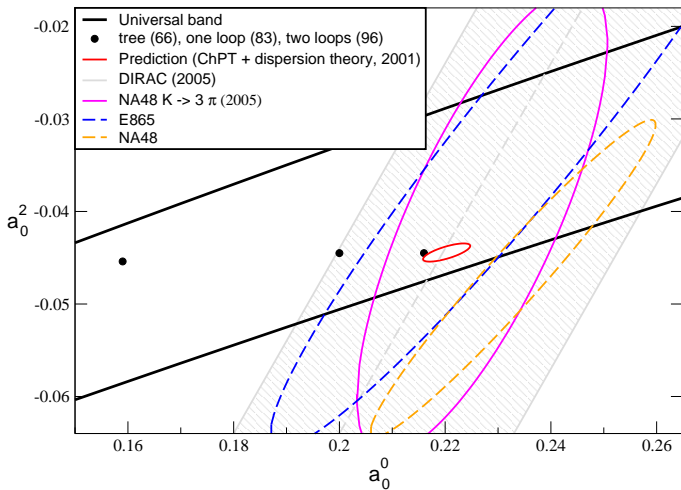
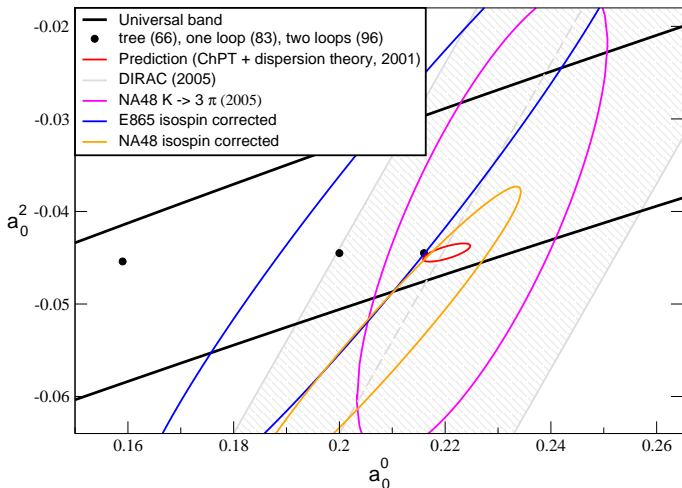
Lattice calculation of a_0^2 (NPLQCD coll.)

Figure from NPLQCD 07

Comparison to lattice and experiment

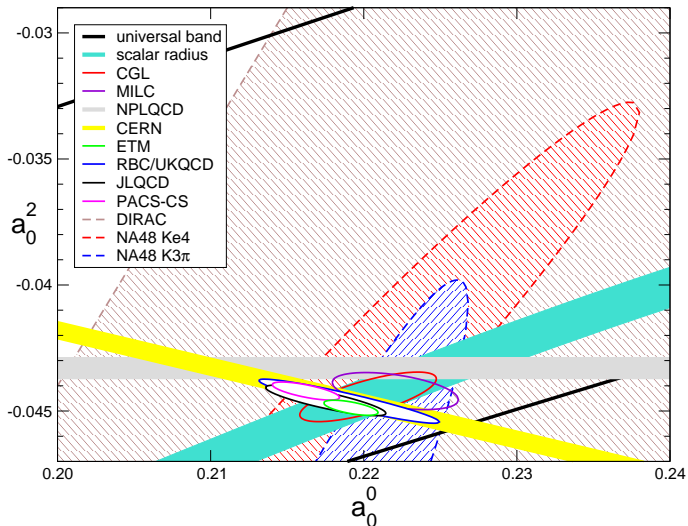


Comparison to lattice and experiment



isospin breaking corrections recently calculated are essential at this level of precision (cf. Gasser talk)

Comparison to lattice and experiment



Outline

Introduction

Roy equations

Chiral symmetry + dispersive methods

Comparison to lattice and experiment

Extension of the Roy equation analysis*

Phenomenological inputs

D and *F* waves

Constraints on high-energy behaviour

Summary

Roy equations

$$\begin{aligned} \text{Re } t_0^0(s) &= k_0^0(s) + \int_{4M_\pi^2}^{s_{0,1}} ds' K_{00}^{00}(s, s') \text{Im } t_0^0(s') \\ &+ \int_{4M_\pi^2}^{s_{0,1}} ds' K_{01}^{01}(s, s') \text{Im } t_1^1(s') \\ &+ \int_{4M_\pi^2}^{s_{0,1}} ds' K_{00}^{02}(s, s') \text{Im } t_0^2(s') + f_0^0(s) + d_0^0(s) \end{aligned}$$

$$k_0^0(s) = a_0^0 + \frac{s - 4M_\pi^2}{12M_\pi^2} (2a_0^0 - 5a_0^2)$$

$$f_0^0(s) = \sum_{\ell'=0}^2 \sum_{\ell'=0}^1 \int_{s_{0,1}}^{s_{3,2}} ds' K_{0\ell'}^{0\ell'}(s, s') \text{Im } t_{\ell'}^{\ell'}(s')$$

$$d_0^0(s) = \text{all the rest}$$

$$\sqrt{s_0} = 0.8\text{GeV}$$

$$\sqrt{s_1} = 1.15\text{GeV}$$

$$\sqrt{s_2} = 1.7\text{GeV}$$

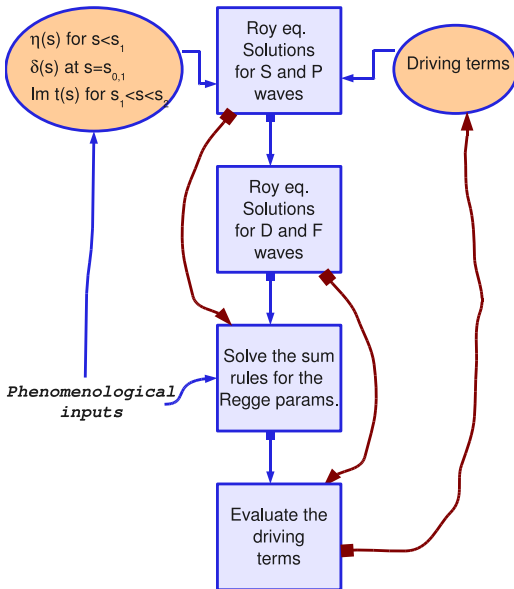
$$\sqrt{s_3} = 2\text{GeV}$$

Extensions and improvements

The analysis done in 2000 (ACGL), which concentrated on the low-energy region can be extended in various directions:

- ▶ High energy part (Regge parameters) had been taken from the literature
 - ▶ new information has become available (e.g. Compete)
 - ▶ various sum rules put constraints on Regge – these had been considered only partially in ACGL
- ▶ D and F waves (\Rightarrow driving terms) taken from the literature
Roy equations can be solved for them too
- ▶ Roy equations valid up to $68M_\pi^2 \sim (1.15\text{GeV})^2$
region $0.8 < \sqrt{s} < 1.15 \text{ GeV}$ can be constrained further
- ▶ more data have become available after 2001 ($\pi N \rightarrow \pi\pi N$ with polarized targets Kaminski, Lesniak and Rybicki) and (measurement of the $e^+e^- \rightarrow \pi^+\pi^-$ cross section, CMD-2, SND, KLOE, and very recently BABAR)

Flowchart of the analysis



Inputs taken from phenomenology

Input phases – need to know:

$$[\sqrt{s_0} = 0.8 \text{ GeV}, \sqrt{s_1} = 1.15 \text{ GeV}]$$

- ▶ three input phase for the S_0 wave:

$$\delta_0^0(s_0) = \begin{cases} 82.3^\circ \pm 3.4^\circ & \text{narrow range (ACGL 00)} \\ 82.3^\circ \begin{smallmatrix} +10^\circ \\ -4^\circ \end{smallmatrix} & \text{broad range (CCL 06)} \end{cases}$$

$$\delta_0^0(4M_K^2) = 185^\circ \pm 10^\circ$$

$$\delta_0^0(s_1) = 260^\circ \pm 10^\circ$$

- ▶ two input phases for the P wave

$$\delta_1^1(s_0) = (108.9 \pm 2)^\circ$$

$$\delta_1^1(s_1) = (166.5 \pm 2)^\circ$$

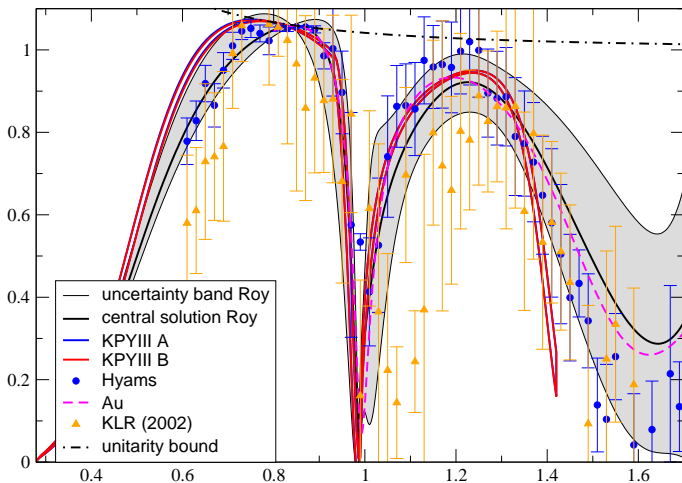
Conservative range: $e^+e^- \rightarrow \pi^+\pi^-$ data more precise

- ▶ **no input phase for the S_2 wave** – once the scattering length a_0^2 and the other S and P waves are fixed, no degree of freedom left in this wave

Inputs taken from phenomenology

Imaginary parts:

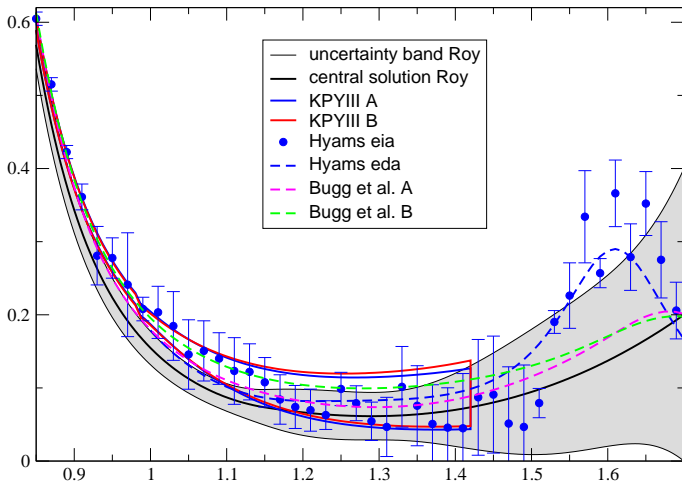
$$\text{Im}t_0^0$$



Inputs taken from phenomenology

Imaginary parts:

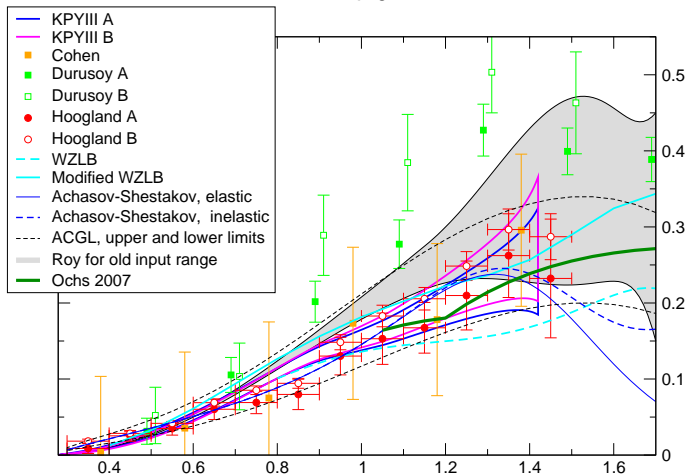
$$\text{Im}t_1^1$$



Inputs taken from phenomenology

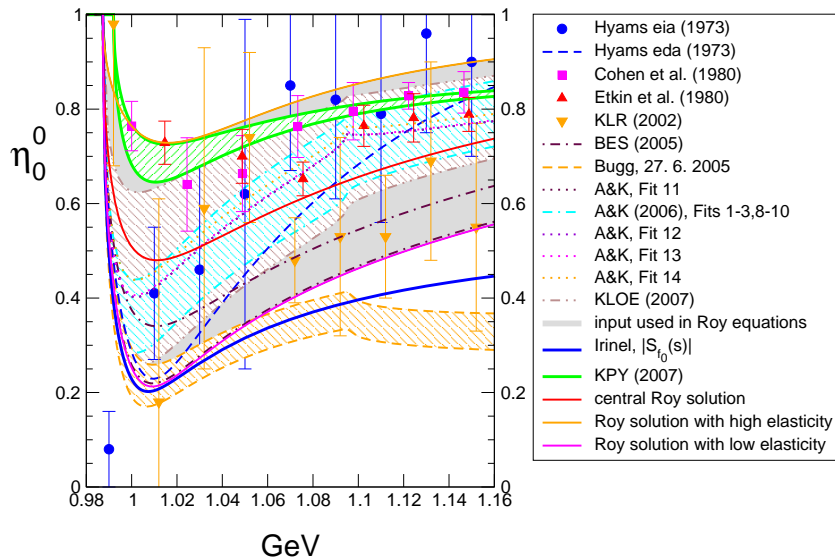
Imaginary parts:

Imt20



Inputs taken from phenomenology

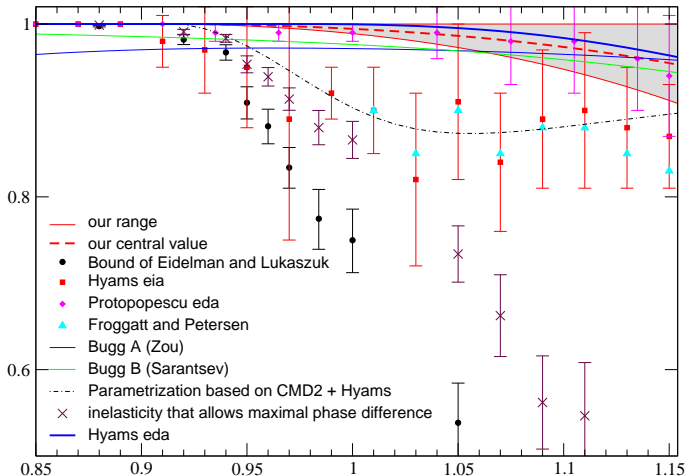
Inelasticities:



Inputs taken from phenomenology

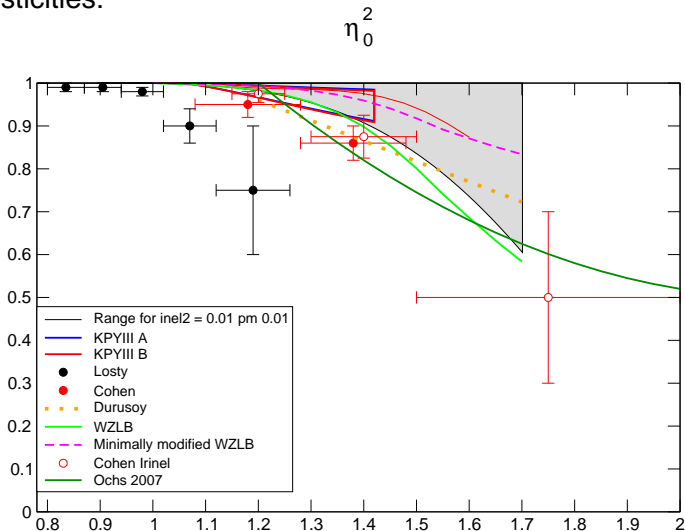
Inelasticities:

eta11

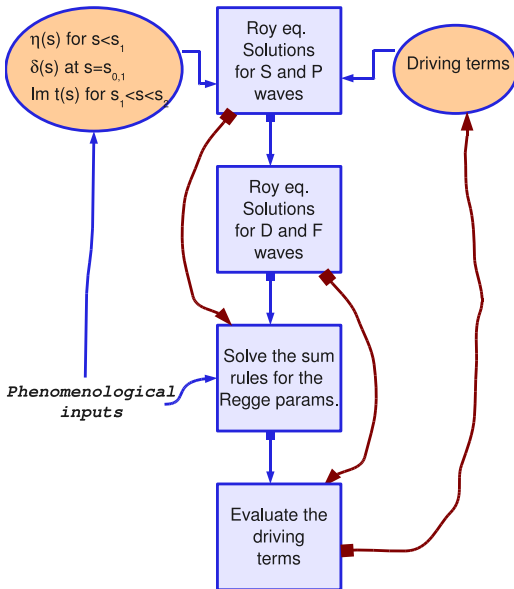


Inputs taken from phenomenology

Inelasticities:



Flowchart of the analysis

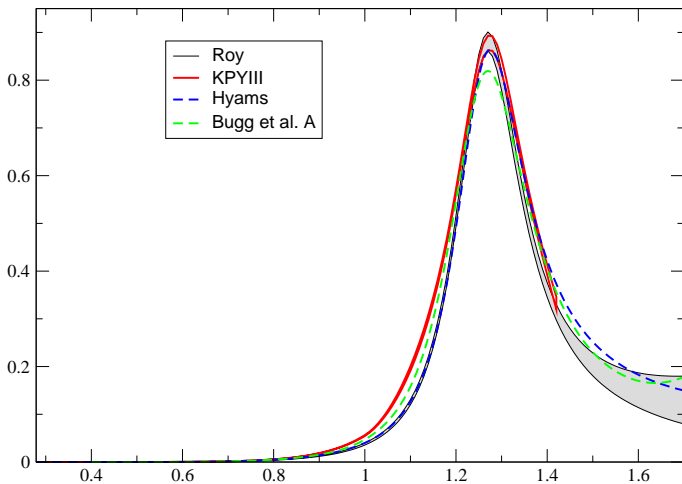


Roy equations for D and F waves

$$\begin{aligned}
 \text{Re } t_2^0(s) &= + \int_{4M_\pi^2}^{s_1} ds' K_{22}^{00}(s, s') \text{Im } t_2^0(s') \\
 &+ \int_{4M_\pi^2}^{s_1} ds' K_{23}^{01}(s, s') \text{Im } t_3^1(s') \\
 &+ \int_{4M_\pi^2}^{s_1} ds' K_{22}^{02}(s, s') \text{Im } t_2^2(s') + f_2^0(s) + d_2^0(s) \\
 f_2^0(s) &= \sum_{l'=0}^2 \sum_{\ell'=0}^1 \int_{s_1}^{s_2} ds' K_{2\ell'}^{0l'}(s, s') \text{Im } t_{\ell'}^l(s') \\
 d_2^0(s) &= \text{S, P, G and higher waves, high energy}
 \end{aligned}$$

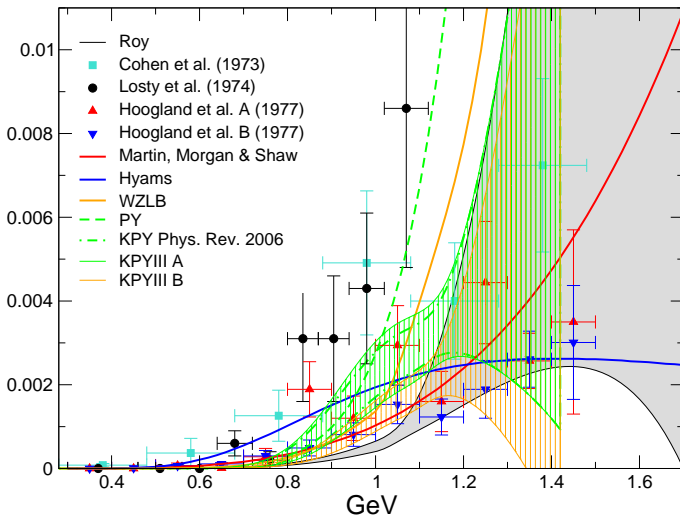
Here the “driving terms” dominate the rhs at low energy: the S and P wave contributions fix to a large extent the D , F and higher waves

Roy equations for D and F waves

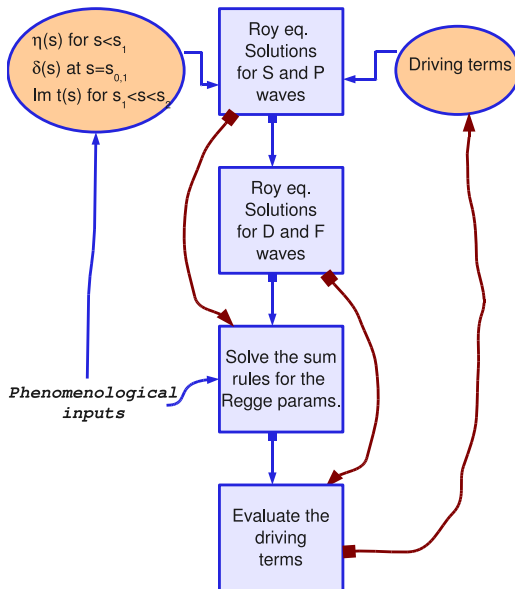
 $\text{Im}t_2^0$ 

Roy equations for D and F waves

$$\text{Im}t_2^2$$



Flowchart of the analysis



Sum rules and asymptotic behaviour

Roy equations do not account for all known constraints:

- in the $I_t = 1$ channel, one subtraction less is necessary

⇒ Olsson sum rule

$$2a_0^0 - 5a_0^2 = \frac{M_\pi^2}{8\pi^2} \int_{4M_\pi^2}^{\infty} ds \frac{2 \operatorname{Im} T^0(s, 0) + 3 \operatorname{Im} T^1(s, 0) - 5 \operatorname{Im} T^2(s, 0)}{s(s - 4M_\pi^2)}$$

- extend the sum rule to any $t \leq 0$

$$\int_{4M_\pi^2}^{\infty} ds \frac{2 \operatorname{Im} \bar{T}^0(s, t) + 3 \operatorname{Im} \bar{T}^1(s, t) - 5 \operatorname{Im} \bar{T}^2(s, t)}{12 s(s + t - 4M_\pi^2)} - \int_{4M_\pi^2}^{\infty} ds \frac{(s - 2M_\pi^2) \operatorname{Im} T^1(s, 0)}{s(s - 4M_\pi^2)(s - t)(s + t - 4M_\pi^2)} = 0$$

- crossing symmetry not fully implemented

⇒ one t -dependent sum rule in each I_t channel
which **do not involve S and P waves**

Regge parameters

At asymptotic energies, the behaviour of the imaginary parts for fixed l_t can be described by Regge formulae

$$\text{Im}T^{l_t=0}(s, t) = \beta_P(t) \left(\frac{s}{s_1}\right)^{\alpha_P(t)} + B \log^2(s/s_B) + \beta_f(t) \left(\frac{s}{s_1}\right)^{\alpha_f(t)}$$

$$\text{Im}T^{l_t=1}(s, t) = \beta_\rho(t) \left(\frac{s}{s_1}\right)^{\alpha_\rho(t)}$$

$$\text{Im}T^{l_t=2}(s, t) = \beta_e(t) \left(\frac{s}{s_1}\right)^{\alpha_e(t)}$$

The COMPETE collaboration offers a phenomenological determination of these parameters

Peláez and Ynduráin have also determined these parameters independently, specifically for $\pi\pi$ scattering

Regge parameters

Our approach:

- the trajectories $\alpha_i(t)$ are well known phenomenologically
- the low-energy contribution to the integrals are determined by the solution to the Roy equations

⇒ use the four sum rules to determine the residues $\beta_i(t)$

Example: Olsson sum rule

$$2a_0^0 - 5a_0^2 = \frac{M_\pi^2}{8\pi^2} \int_{4M_\pi^2}^{s_2} ds \text{ [partial w.]} + \beta_\rho(0) \frac{3M_\pi^2}{4\pi^2} \int_{s_2}^{\infty} ds \frac{(s/s_1)^{\alpha_\rho(0)}}{s(s - 4M_\pi^2)}$$

Regge parameters

- In this way we tune the Regge residues such that the integrals below and above 1.7 GeV match exactly
- Moreover we also make sure that the imaginary parts (cross sections) are continuous at 1.7 GeV
- In order to do this we multiply the Regge representations with “preasymptotic terms”:

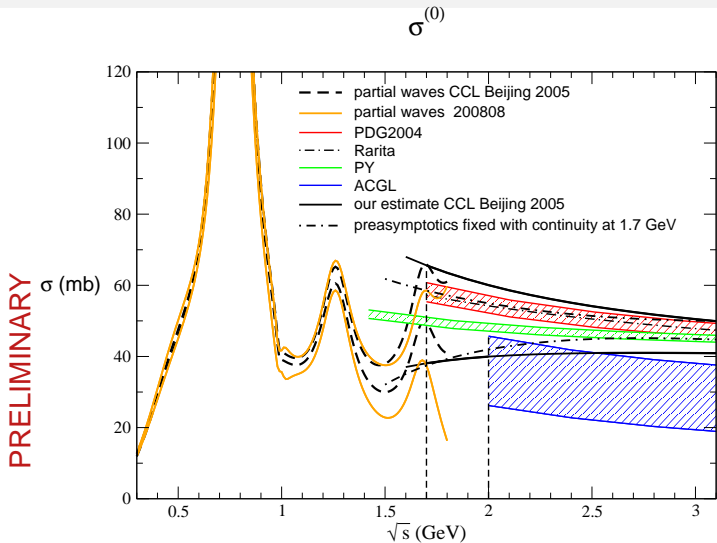
$$\text{Im} T^l(s, t) = \text{Im} T_{\text{Regge}}^l(s, t) \left(1 + r_l \frac{s}{\bar{s}} \right)$$

and tune the parameter r_l accordingly

- We also fix the t -dependence of the residues (profile) by continuity

$$\beta_X(t) \equiv \beta_X(0) b_X(t)$$

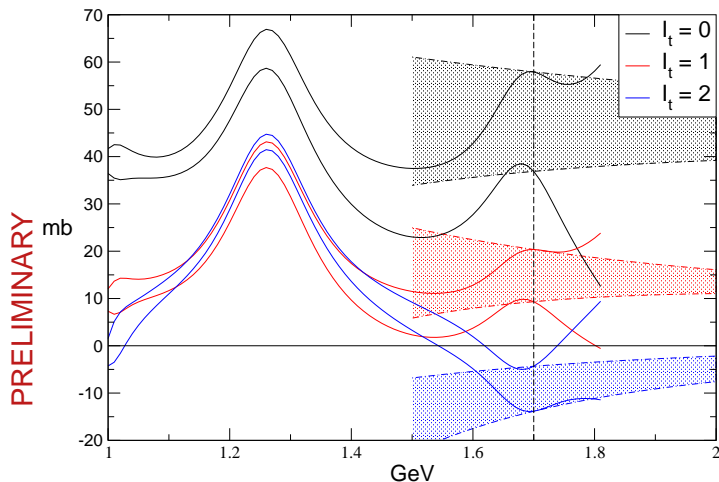
Regge parameters



Work in progress with I. Caprini and H. Leutwyler

Regge parameters

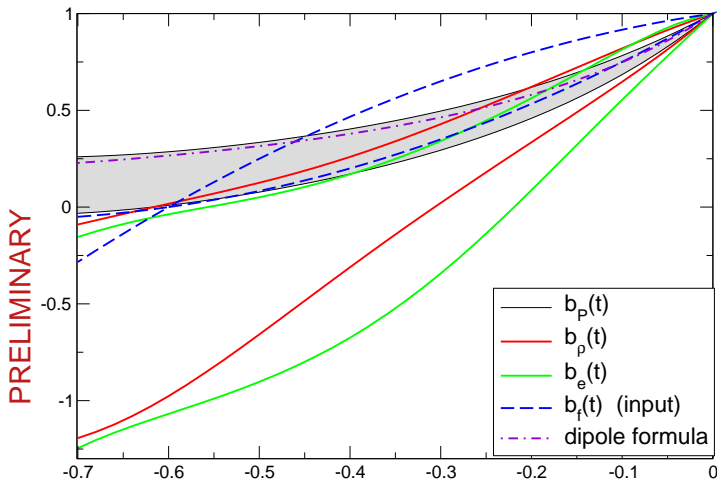
Total cross section



Work in progress with I. Caprini and H. Leutwyler

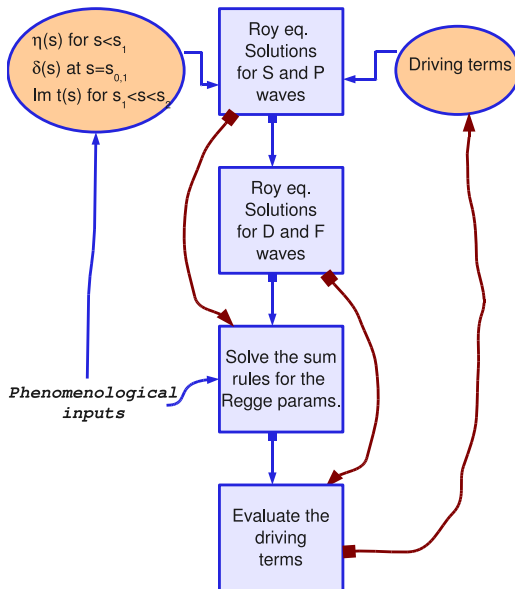
Regge parameters

Profiles of the Regge residues



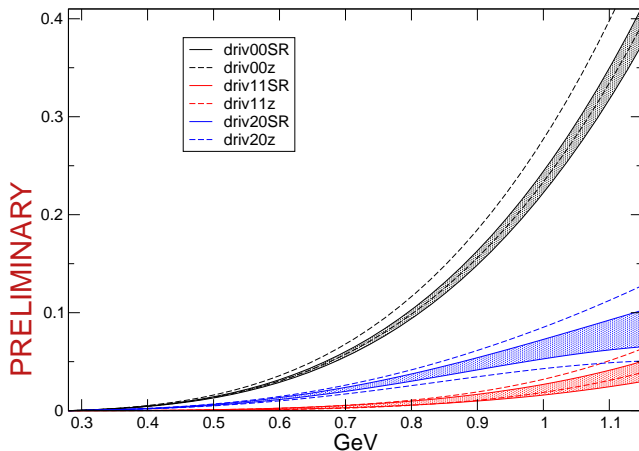
Work in progress with I. Caprini and H. Leutwyler

Flowchart of the analysis



Driving terms

The iterative determination of the driving terms converges immediately:



Work in progress with I. Caprini and H. Leutwyler

Outline

Introduction

Roy equations

- Chiral symmetry + dispersive methods

- Comparison to lattice and experiment

Extension of the Roy equation analysis*

- Phenomenological inputs

- D and F waves

- Constraints on high-energy behaviour

Summary

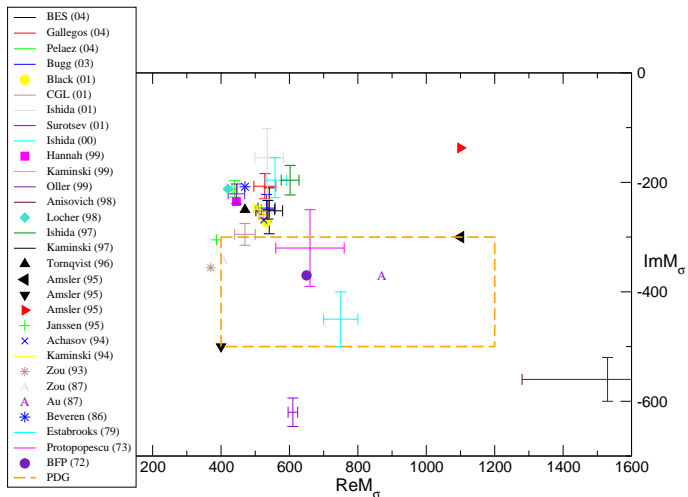
Summary

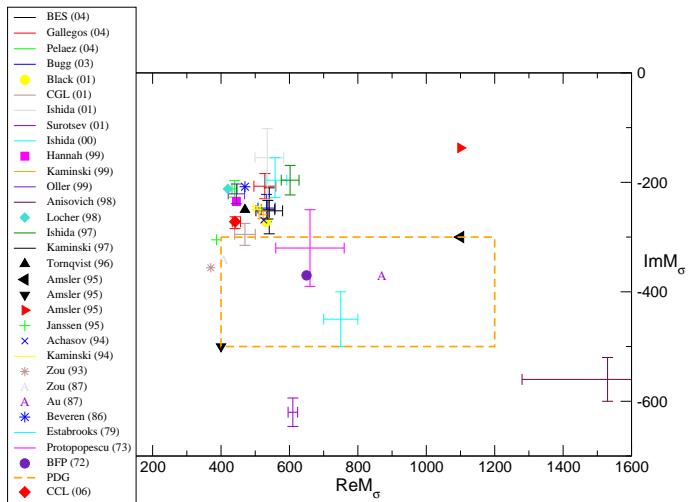
- ▶ the $\pi\pi$ scattering amplitude at low energy can be predicted with **high accuracy** thanks to a combination of **chiral symmetry** and **dispersion relations**
- ▶ **experiments (E865, DIRAC and NA48)** are reaching the same level of accuracy
- ▶ **lattice calculations** of \bar{l}_3 and \bar{l}_4 essentially determine the two subtractions constants and are competitive with phenomenological determinations
- ▶ a **direct lattice calculation** of a_0^2 with comparable accuracy is already available (NPLQCD) – a_0^0 is more difficult
- ▶ I have presented an extension of the Roy equation analysis to **higher energy** and **higher partial waves**
- ▶ **no significant changes** at low energy, but a much better control on the high-energy inputs

Outline

The σ resonance

FLAG color coding

The σ in the PDG

The σ in the PDG

Roy representation of S_0^0

$$S_0^0(s) = 1 - 2\sqrt{\frac{4M_\pi^2}{s} - 1}t_0^0(s), \quad 0 \leq s \leq 4M_\pi^2$$

where t_0^0 is given by a double-subtracted, crossing symmetric dispersion relation

$$t_0^0(s) = a + (s - 4M_\pi^2)b + \int_{4M_\pi^2}^{\Lambda^2} ds' \left\{ K_0(s, s') \operatorname{Im} t_0^0(s') \right. \\ \left. + K_1(s, s') \operatorname{Im} t_1^1(s') + K_2(s, s') \operatorname{Im} t_0^2(s') \right\} + d_0^0(s)$$

$$a = a_0^0, \quad b = (2a_0^0 - 5a_0^2)/(12M_\pi^2)$$

$$K_0(s, s') = \frac{1}{\pi(s' - s)} + \frac{2 \ln((s + s' - 4M_\pi^2)/s')}{3\pi(s - 4M_\pi^2)} - \frac{5s' + 2s - 16M_\pi^2}{3\pi s'(s' - 4M_\pi^2)}$$

Roy representation of S_0^0

$$S_0^0(s) = 1 - 2\sqrt{\frac{4M_\pi^2}{s} - 1}t_0^0(s), \quad 0 \leq s \leq 4M_\pi^2$$

Unitarity implies that: $S_0^0 I(s + i\epsilon) = [S_0^0 I(s - i\epsilon)]^{-1}$

The second sheet is reached by analytic continuation crossing the real axis from above: (for ϵ infinitesimally small)

$$S_0^0 II(s - i\epsilon) = S_0^0 I(s + i\epsilon) = [S_0^0 I(s - i\epsilon)]^{-1}$$

By analytic continuation, it is then true everywhere that

$$S_0^0 II(s) = [S_0^0 I(s)]^{-1}$$

Poles on the second sheet correspond to zeros on the first sheet!

Method to determine the pole position

- ▶ Roy equations provide an explicit representation of t_0^0 on the first sheet, in terms of the imaginary parts of the partial waves on the real axis and two subtraction constants:

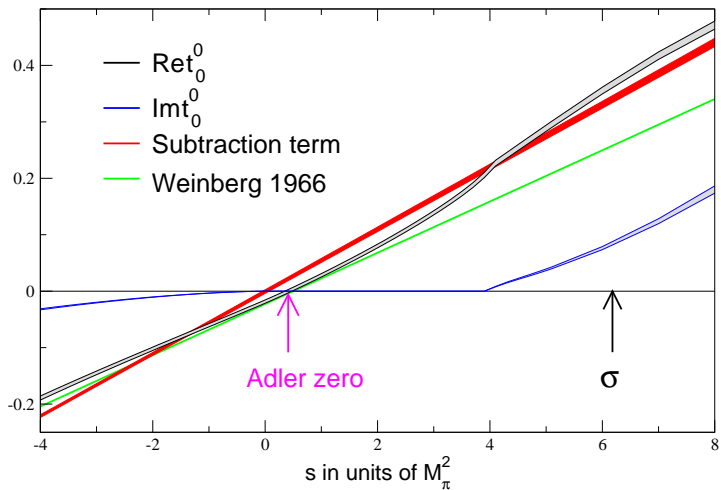
$$t_0^0(s) = a + (s - 4M_\pi^2) b + \int_{4M_\pi^2}^{\Lambda^2} ds' K_0(s, s') \text{Im } t_0^0(s') + \dots$$

- ▶ Unitarity implies that the S-matrix on the second sheet is equal to the inverse of the S-matrix on the first sheet

$$S_0^{0''}(s) = [S_0^{0'}(s)]^{-1}$$

- ▶ Using as input the imaginary parts of the partial waves and the two S-wave scattering lengths one can determine the position of the poles of the S-matrix on the second sheet

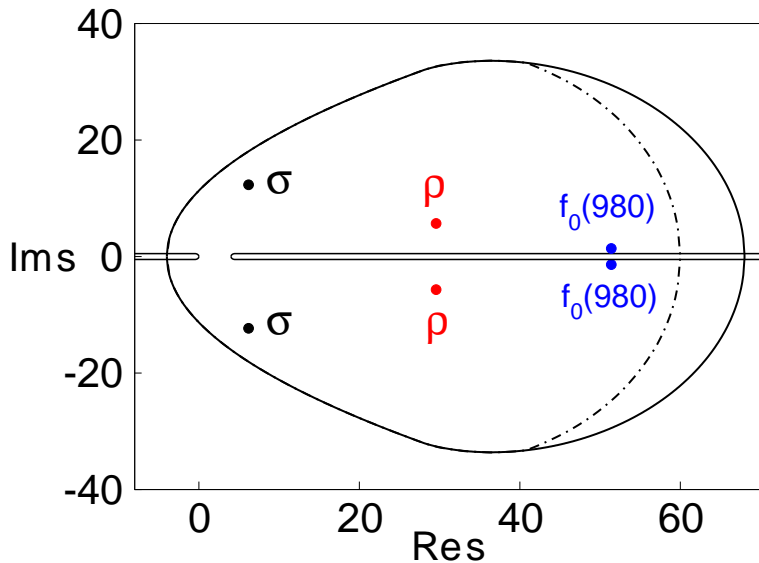
Importance of the scattering lengths



Zeros of S_0^0 (and S_1^1)

Input: the imaginary parts from Roy solutions below 1.15 GeV and the central values of the two scattering lengths (CHPT) we find two pairs of zeros

$$m_\sigma^2 = (6.2 \pm i 12.3) M_\pi^2 \quad m_{f_0}^2 = (51.4 \pm i 1.4) M_\pi^2$$

Zeros of S_0^0 (and S_1^1)

Zeros of S_0^0 (and S_1^1)

Input: the imaginary parts from Roy solutions below 1.15 GeV and the central values of the two scattering lengths (CHPT) we find two pairs of zeros

$$m_\sigma^2 = (6.2 \pm i 12.3) M_\pi^2 \quad m_{f_0}^2 = (51.4 \pm i 1.4) M_\pi^2$$

Error analysis: [at fixed a_0^0 , a_0^2 and $\delta_A \equiv \delta_0^0(0.8\text{GeV})$]

$$m_\sigma = 441 \pm 4 - i(272 \pm 6) \text{ MeV} + (-2.4 + i3.8)\Delta a_0^0 \\ + (0.8 - i4.0)\Delta a_0^2 + (5.3 + i3.3)\Delta\delta_A$$

$$\Delta a_0^0 = \frac{a_0^0 - 0.220}{0.005} \quad \Delta a_0^2 = \frac{a_0^0 + 0.0444}{0.001} \quad \Delta\delta_A = \frac{\delta_A - 82.3}{3.4}$$

Zeros of S_0^0 (and S_1^1)

Input: the imaginary parts from Roy solutions below 1.15 GeV and the central values of the two scattering lengths (CHPT) we find two pairs of zeros

$$m_\sigma^2 = (6.2 \pm i 12.3) M_\pi^2 \quad m_{f_0}^2 = (51.4 \pm i 1.4) M_\pi^2$$

Error analysis: [at fixed a_0^0 , a_0^2 and $\delta_A \equiv \delta_0^0(0.8\text{GeV})$]

$$m_\sigma = 441 \pm 4 - i(272 \pm 6) \text{ MeV} + (-2.4 + i3.8)\Delta a_0^0 \\ + (0.8 - i4.0)\Delta a_0^2 + (5.3 + i3.3)\Delta\delta_A$$

$$\Delta a_0^0 = \frac{a_0^0 - 0.220}{0.005} \quad \Delta a_0^2 = \frac{a_0^0 + 0.0444}{0.001} \quad \Delta\delta_A = \frac{\delta_A - 82.3}{3.4}$$

$$m_\sigma = 441^{+16}_{-8} - i272^{+13}_{-9}$$

Different inputs

- ▶ The extension of the Roy equation analysis from 0.8 to 1.15 GeV has no impact on m_σ . Using CGL (01) we get

$$m_\sigma^{\text{CGL}}(\text{model indep.}) = 439.4 - i274.5 \text{ MeV}$$

$$m_\sigma^{\text{CGL}}(\text{param.-dep.}) = 470 \pm 30 - i295 \pm 20 \text{ MeV}$$

Different inputs

- ▶ The extension of the Roy equation analysis from 0.8 to 1.15 GeV has no impact on m_σ . Using CGL (01) we get

$$m_\sigma^{\text{CGL}}(\text{model indep.}) = 439.4 - i274.5 \text{ MeV}$$

$$m_\sigma^{\text{CGL}}(\text{param.-dep.}) = 470 \pm 30 - i295 \pm 20 \text{ MeV}$$

- ▶ Using a phenomenological representation of the $\pi\pi$ scattering amplitude [Pelaéz and Ynduráin (05)] we obtain

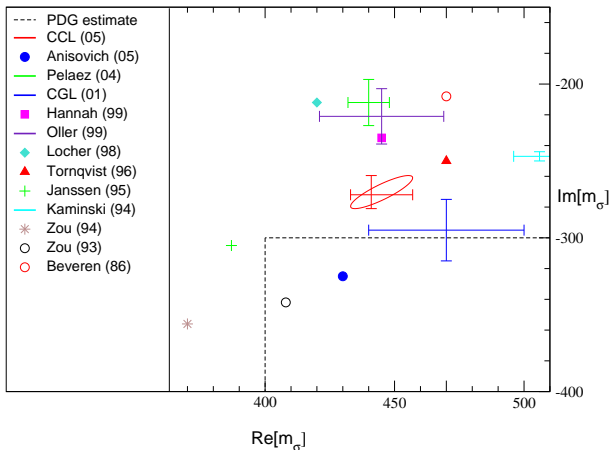
$$m_\sigma^{\text{PY}} = 445 - i241 \text{ MeV}$$

Our formula which describes the dependence on the main three input parameters reproduces this result:

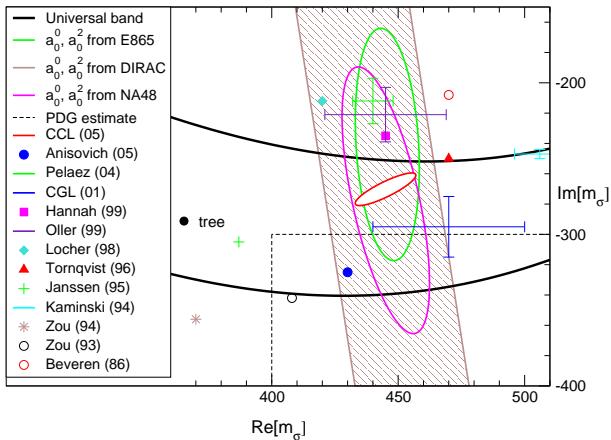
$$a_0^0(PY) = 0.23, \quad a_0^2(PY) = -0.048, \quad \delta_A(PY) = 90.9^\circ$$

$$\Rightarrow m_\sigma = 447 - i242 \text{ MeV}$$

Comparison to PDG and experimental information



Comparison to PDG and experimental information



Outline

The σ resonance

FLAG color coding

Color coding

Already used sometimes by lattice people in summaries
Our current working hypothesis

Color coding

Already used sometimes by lattice people in summaries

Our current working hypothesis

- ▶ chiral extrapolation
 - using NLO or NNLO CHPT formulae
 - phenomenologically motivated chiral extrap.
 - no chiral extrapolation

Color coding

Already used sometimes by lattice people in summaries

Our current working hypothesis

- ▶ chiral extrapolation
- ▶ smallest pion mass
 - $\min M_\pi < 300 \text{ MeV}$
 - $\min M_\pi < 400 \text{ MeV}$
 - $\min M_\pi > 400 \text{ MeV}$

Color coding

Already used sometimes by lattice people in summaries

Our current working hypothesis

- ▶ chiral extrapolation
- ▶ smallest pion mass
- ▶ finite volume effects
 - volume scaling study (in combination with CHPT)
 - CHPT
 - no assessment of finite volume corrections

Color coding

Already used sometimes by lattice people in summaries

Our current working hypothesis

- ▶ chiral extrapolation
- ▶ smallest pion mass
- ▶ finite volume effects
- ▶ continuum extrapolation
 - $O(a)$ -improved or chiral fermions, at least two a 's, $\min a < 0.1$ fm
 - $O(a)$ -improved or chiral fermions, one $a \lesssim 0.1$ fm
 - larger lattice spacing or no improvement

Color coding

Already used sometimes by lattice people in summaries

Example

	\bar{l}_3	N_f	chiral extrapolation	smallest pion mass	finite volume errors	continuum extrapolation
CERN	3.0(5)(1)	2	●	●	●	●
ETM	3.44(8)(35)	2	●	●	●	●
MILC	1.1(6) $^{+1.0}_{-0.5}$	2+1	●	●	●	●
RBC/UKQCD	3.13(33)(24)	2+1	●	●	●	●
JLQCD/TWQCD	3.44(57) $^{+32}_{-68}$	2	●	●	●	●
PACS-CS	3.14(23)(?)	2+1	●	●	●	●